Introducing Spin-coated ZnO Anti-reflection Coating for CdS/CdTe Solar Cells

Article *in* Journal of Electronic Materials · July 2024

DOI: 10.1007/s11664-024-11260-0

6 authors, including:

Janith Wijesingha
RMIT University
3 PUBLICATIONS **9** CITATIONS
SEE PROFILE

G.K.U.P. Gajanayake
University of Kelaniya
9 PUBLICATIONS **12** CITATIONS
SEE PROFILE

W.A.Vinura Udaraka Wickramasinghe
University of Surrey
2 PUBLICATIONS **0** CITATIONS
SEE PROFILE

Indika De Silva
University of Moratuwa
38 PUBLICATIONS **133** CITATIONS
SEE PROFILE

Journal of Electronic Materials
https://doi.org/10.1007/s11664-024-11260-0

ORIGINAL RESEARCH ARTICLE

Introducing Spin-coated ZnO Anti-reflection Coating for CdS/CdTe Solar Cells

J. R. Wijesingha[1] · G. K. U. P. Gajanayake[2] · W. A. V. U. Wickramasinghe[3] · R. M. T. Damayanthi[1] · G. I. P. De Silva[4] · D. S. M. De Silva[2]

Received: 16 January 2024 / Accepted: 10 June 2024

Abstract

Second-generation solar cells, commonly known as thin-film solar cells, have emerged as promising alternatives to traditional silicon-based first-generation photovoltaic cells. The superstrate configuration is the most widely used structure for constructing thin-film solar cells. Nevertheless, light reflection from the front cover glass surface significantly contributes to energy losses in thin-film solar cells. In this study, a ZnO anti-reflection (AR) coating was introduced using the spin coating technique on a glass/FTO/CdS/CdTe/Cu/Au substrate to improve the power conversion efficiency of the solar cell by reducing front-surface reflectance. The ZnO layer deposited at 3000 rpm in 15 s showed the minimum reflectance and higher transmittance over a wavelength range of 500–900 nm. Further, the thickness of the film under optimal conditions was 63.32 nm, which is compatible with the ideal theoretical AR coating thickness of 65 nm. Comparing the device performance of the CdS/CdTe solar cell with and without AR coating, all tested devices showed an average short-circuit current density improvement of 6.8% and overall enhancement in power conversion efficiency of 9.3%.

Keywords AR coating · CdS/CdTe solar cell · reflectance · spin coating

Introduction

Solar cell or photovoltaic cell technology is rapidly growing and poised to play an important role in global electricity generation in the near future. Even though solar cells have evolved through several generations, first-generation solar cells, made of single- and multi-crystalline silicon, are the most common on the market due to their wide availability and high stability. However, higher manufacturing cost and lower power conversion efficiency (PCE) are key limitations of silicon-based solar cells.[1] Therefore, second-generation cadmium telluride solar cells (CdTe) have become the most prevalent thin film type due to their lower cost and material requirements than traditional Si based solar cells. Additionally, the recorded laboratory-scale PCE of CdTe solar cells is 22.4%, which is competitive with the PCE of single-crystal silicon cells (27.6%).[2,3] Therefore, integrating cost-effectiveness and ongoing research and development efforts to enhance efficiency will position CdTe solar cells as strong competitors to traditional silicon-based cells.

The PCE of these thin-film solar cells is limited mainly due to the reflectance of light from their front surface. Thus, introducing ultrathin and transparent anti-reflection (AR) film coatings can ensure high PCE by reducing the reflectance of light from the front surface of the solar cells. Previous studies have employed different kinds of materials such as ZnS, SiO_2, ZnO, MgO, and TiO_2 as AR coatings for photovoltaic cells using various deposition techniques. Gangopadhyay et al.[4] introduced a low-cost ZnS AR coating on monocrystalline silicon solar cells using the chemical bath deposition (CBD) technique, and reported that I_{sc} and PCE improved by 6.5% and 5%, respectively. Similarly, Li et al.[5] found that after introducing an electron beam-evaporated SiO_2 AR coating for silicon solar cells, the PCE was slightly improved from 17.48% to 17.8%. Sagar and Rao[6] reported

✉ J. R. Wijesingha
j.randima0@gmail.com

1 Department of Electrical Engineering, University of Moratuwa, Katubedda, Sri Lanka

2 Department of Chemistry, University of Kelaniya, Kelaniya, Sri Lanka

3 Advanced Technology Institute, University of Surrey, Guildford, UK

4 Department of Materials Science and Engineering, University of Moratuwa, Katubedda, Sri Lanka

Published online: 02 July 2024

that implementing radio-frequency (RF)-sputtered MgO and Al_2O_3 AR coatings on silicon solar cells increased their PCE from 8.33% to 9.86% and 8.38% to 9.13%, respectively. Pakhuruddin et al.[7] investigated RF-sputtered ZnO AR coating on microcrystalline silicon solar cells, which provided minimum reflectance at 600 nm of 2%, while liquid-phase-deposited (LPD) TiO_2 grown on silicon substrate exhibited an average minimum reflectance of 2.7% at a wavelength range of 400–800 nm as reported by Wang et al.[8]

Research on single-layer AR coating for superstrate CdTe solar cells is notably rare in the literature. However, Kaminski et al.[9] undertook an experiment on quadruple-layer AR coating comprising SiO_2 and ZrO_2 for CdS/CdTe solar cells through DC magnetron sputtering. Their work yielded a 3% increase in current density, achieving a minimum reflectance of 5% within the wavelength range of 500–600 nm. Employing the aforementioned AR coating materials and deposition technique, Law et al.[10] fabricated a six-layer AR coating for CdSeTe/CdTe solar cells, yielding 3.45% enhancement in current density and 3.54% improvement in PCE. However, the total thickness of the AR coating of both studies was greater than 250 nm, which can lead to a reduction in the transmittance of the whole cell. In contrast to multilayer AR coatings, with careful selection of the appropriate AR coating material and thickness, a single-layer AR coating may provide a significant improvement in current density and PCE with minimal cost.

The thin-film CdS/CdTe solar cells are developed using the superstrate configuration rather than the substrate configuration[11] to increase the light absorption, protection, and durability of the device. Therefore, the AR coating can be deposited on the top of the non-conductive side of the glass substrate before fabricating the solar cells or alternatively on the top of the complete device. However, the AR coating on the non-conductive side of the glass substrate prior to device fabrication can damage the AR coating during the solar cell material deposition process. Hence, it is advantageous to apply the AR coating after the solar cell has been fabricated.

In the present study, low-cost, nontoxic, wide-bandgap ($E_g \sim 3.37$ eV) ZnO was tested as the AR coating for CdS/CdTe solar cells due to its excellent transmittance in visible light, low resistance, optimum refractive index ($n \sim 2.0$), and ability to grow using low-temperature deposition techniques.[12,13] To achieve cost-effective deposition of ultrathin and uniform ZnO AR coating on a non-conductive substrate at low temperatures, we chose the spin coating technique for the experiment.

Theoretical Evaluation

Single-Layer AR Coating Design

Designing single-layer AR coating using theoretical calculations is advantageous prior to the fabrication. AR coatings are designed considering the relative phase shift between the incident beam reflected at the upper and lower surfaces of the AR coating. Therefore, the optical thickness of the AR coating must be equal to a quarter of the incident light wavelength for zero reflectance, as indicated in Eq. 1.[14]

$$n_{AR}t = \frac{\lambda}{4} \tag{1}$$

Since the reflected beams have a180° phase shift, destructive interference cancels out both reflected beams before they exit the surface (Fig. 1).

The wavelength range considered in this experiment was 300–900 nm. However, a single-layer AR coating meets the minimum reflectivity only at a single wavelength, not over the whole wavelength range. Consequently, the initial design focused on a narrow wavelength band where the higher radiation intensities of the solar spectrum occur. However, this approach is crucial for obtaining relatively low reflectivity in a specific wavelength range to achieve maximum power conversion efficiency of the solar cells.

Since the CdS window layer absorbs a higher portion of incident light at the 300–520 nm range before reaching the

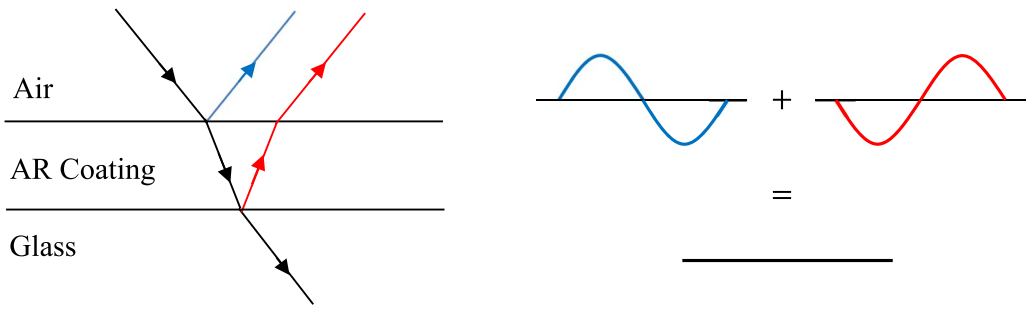

Fig. 1 Destructive interference between reflected beams.

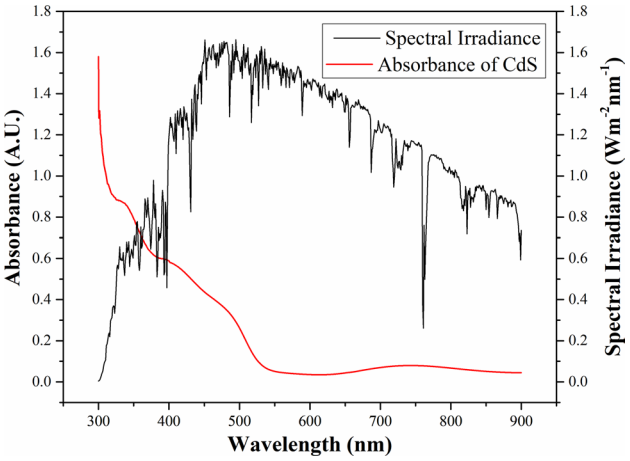

Fig. 2 Absorbance spectrum of CdS and solar irradiance spectrum.

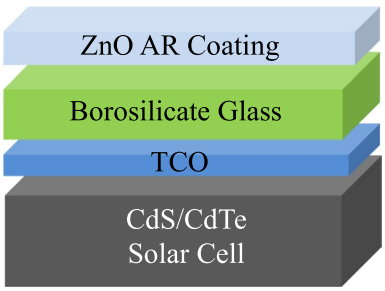

Fig. 3 CdS/CdTe solar cell structure with AR coating.

CdTe absorber layer, this study focused on the 500–900 nm wavelength range (Fig. 2) to minimize the front surface reflectivity and enhance the PCE of solar cell. According to Fig. 2, the maximum radiation intensity of the solar spectrum occurs between 450 nm and 550 nm wavelength. Therefore, obtaining minimum reflectance at 520 nm is better for the initial design of the AR coating. In addition, according to Eq. 1, the thickness of the AR coating should be around 65 nm, assuming the refractive index of ZnO is about 2.[12]

Experimental Details

Deposition of the ZnO Layer

The thin-film ZnO layer was deposited on the borosilicate glass substrate (2.2 × 2.5 cm^2) as shown in Fig. 3, using spin coating.

Initially, the glass substrates were subjected to a cleaning process. Here, they were wiped with detergent, and then ultrasonically cleaned samples were immersed in acetone, methanol, and 2-propanol at a temperature of 80°C for 5 min, respectively, and finally air-dried. Prior to the deposition of the ZnO thin film, a saturated ZnO solution was prepared by dissolving 1.7 g of zinc acetate ($Zn(CH_3COO)_2$) in 25 ml of methanol followed by gravity-filtration. Before the spin coating process, borosilicate substrates were subjected to cleaning by O_2 plasma, which is a common technique for surface cleaning prior to bonding. Afterward, a set of thin-film ZnO samples was spin coated at speeds of 1000–3500 rpm in steps of 500 rpm (the samples were denoted as S1, S2, S3, S4, S5, and S6) while keeping other parameters constant. The ZnO thin layer was developed by adding 0.75 ml of the $Zn(CH_3COO)_2$ dropwise into the center of the substrate immediately upon the start of spinning, which was maintained for 15 s. After the deposition, samples were heat-treated at 100°C for 120 min at atmospheric pressure in a tube furnace (GSL-1700X).

After the optimized deposition conditions were determined, the thin-film ZnO coating was fabricated on a non-conducting glass substrate of the laboratory-developed glass/fluorine-doped tin oxide (FTO)/CBD-CdS/CSS [close-spaced sublimation]-CdTe/Cu/Au solar cell.[15]

Characterization

The absorbance and transmittance spectra of the ZnO layers were obtained by UV–visible spectroscopy (PerkinElmer Lambda 365 UV/Vis spectrophotometer) in the wavelength range of 300–900 nm. The front surface reflectance spectrum of the coated substrate was measured by a Bentham external quantum efficiency (EQE) setup (PVE300) to identify the best rpm value of the spin coater in order to achieve minimal reflectance. Moreover, the thickness of the ZnO coating was measured by a profilometer (DektacXT). Then, atomic force microscopy (AFM) (Bruker Dimension Edge AFM) and energy-dispersive x-ray spectroscopy (EDAX Element) were performed to analyze the RMS roughness and identify the composition of the grown material of the optimized sample, respectively. Ultimately, the performance of the glass/FTO/CdS/CdTe/Cu/Au solar devices, with and without the AR coating, was measured under AM 1.5 illumination conditions (100 mW cm^{-2}) using a solar simulator (PEC-L12).

Results and Discussion

Theoretical Background of the Formation of ZnO

The chemical reaction of zinc acetate ($Zn(CH_3COO)_2$ (s)) and methanol (CH_3OH (aq)) is an esterification reaction that produces byproducts of methyl acetate (CH_3COOCH_3 (aq)) and zinc hydroxide ($Zn(OH)_2$ (aq)), as represented in Eq. 2.

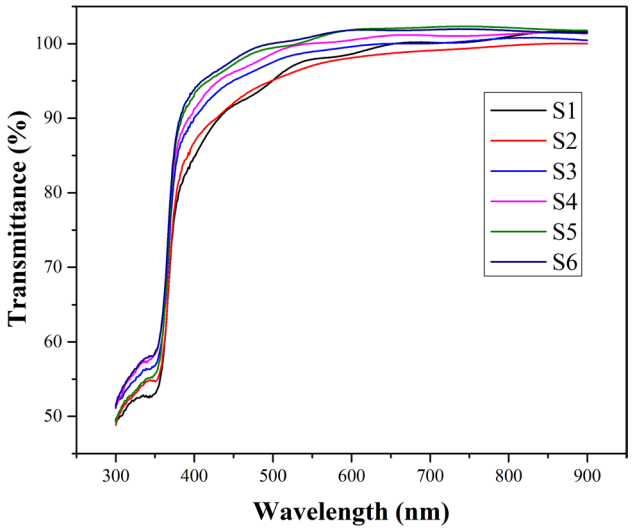

Fig. 4 Optical transmittance vs. wavelength plot of the ZnO AR coatings (S1 to S6).

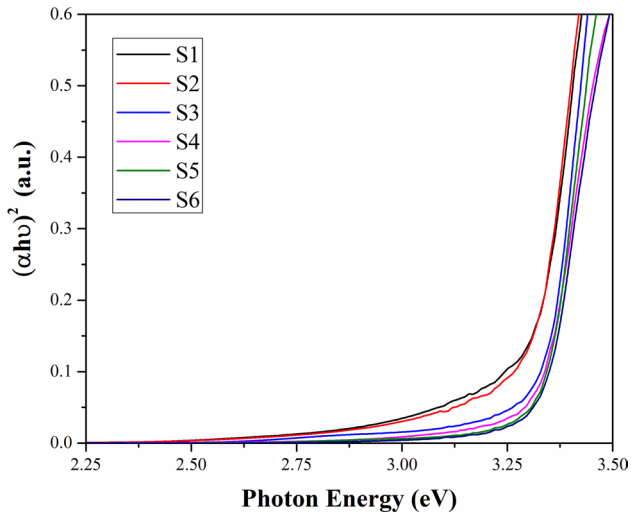

Fig. 5 Tauc plot for the ZnO AR coatings S1 to S6.

$$Zn(CH_3COO)_2(s) + 2\ CH_3OH(aq) \rightarrow 2\ CH_3COOCH_3(aq) + Zn(OH)_2(aq) \quad (2)$$

Since the boiling point of CH_3COOCH_3 (aq) is about 57°C[16] at standard atmospheric pressure (1 atm), at temperatures above 57°C, methyl acetate is vaporized. Here, when the spin-coated material is subjected to thermal annealing at 100°C, ZnO (s) film is formed by dehydration of $Zn(OH)_2$ (aq) (Eq. 3).

$$Zn(OH)_2(aq) \rightarrow ZnO(s) + H_2O\ (g) \quad (3)$$

Optical Properties

The optical transmittance values of the ZnO layers grown under the different spin rates are shown in Fig. 4. Here, the ZnO layer deposited at low spin rates (S1 and S2) showed over 95% transmittance of light in the wavelength range of 500–900 nm. However, when the spin rate increased, the maximum transmittance (> 95%) occurred at a broader wavelength range. Consequently, the samples obtained at high spin rates (S5 and S6) showed over 95% transmittance of light in the wide optical range of 400–900 nm.

Figure 5 presents the relevant Tauc plots for the growth of ZnO samples deposited at different spin rates. The ideal AR coating shows minimal absorbance across the spectrum, allowing most incident light to pass through the layer. The theoretical bandgap energy of ZnO is about 3.37 eV,[17] corresponding to a wavelength of 368 nm. Specifically, ZnO is more transparent to light at wavelengths longer than 368 nm and absorbs light at shorter wavelengths (less than 368 nm). Table I illustrates the energy bandgap values (E_g) of samples S1 to S6 determined from the Tauc plots. It is observed that the bandgap value increased slightly in proportion to the spin rate. Samples S1 and S2 have much lower bandgap values than their theoretical value (3.37 eV). However, the bandgaps of S4 to S6 reached closer to the theoretical value of ZnO.

Since this study aimed to obtain maximum transmittance within the wavelength range of 450–550 nm, where the solar spectrum exhibits higher intensity, the bandgap of ZnO was accurately aligned with the requirement. Samples S5 and S6, for which the ZnO layers were coated at 3000 rpm and 3500 rpm, respectively, and had higher light transmittance, were identified as the best AR coatings in this study. After identifying samples S5 and S6 as possible AR coatings for the solar cell, all samples were subjected to reflectance analysis to determine the selected AR coating deposition parameters.

The reflectance spectrum of samples S1 to S6 in the wavelength range of 300–1000 nm is shown in Fig. 6. The highest intensity peak of reflectance was observed at a particular wavelength due to the phenomenon of constructive interference. The constructive interference occurs when waves reflected from the front and back surfaces are in the same phase and result in an intense peak in the spectrum.

Table I The energy bandgap of samples S1 to S6 with respect to spin rate

Sample	S1	S2	S3	S4	S5	S6
Spin rate (rpm)	1000	1500	2000	2500	3000	3500
Energy bandgap (eV)	3.29	3.28	3.31	3.32	3.32	3.32

As shown in Fig. 6, lower reflectance was observed for samples S5 and S6 at a wavelength of 375 nm. Sample S5 exhibited the lowest reflectance over the wavelength range of 500–900 nm. The lower the reflectance, the better the light transmission; therefore, S5 was identified as the optimal AR coating among the studied samples.

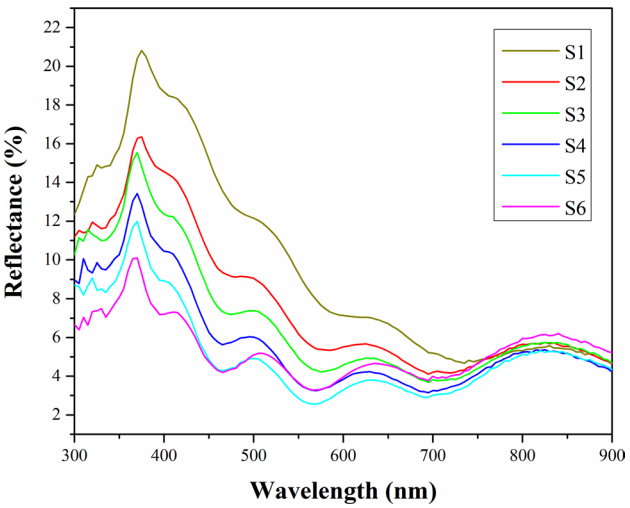

Fig. 6 Reflectance vs. wavelength plot of the ZnO AR coatings S1 to S6.

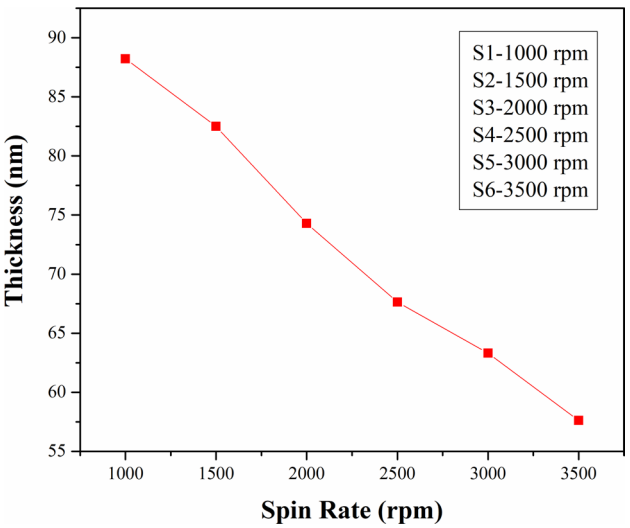

Fig. 7 Thickness of the ZnO AR coating vs. spin rate of deposition.

Variation in AR Coating Thickness

Figure 7 shows the variation in the thickness of the ZnO layer with the spin rate. The thickness of the AR coating decreased (from around 90 nm to 55 nm) with the increase in the spin rate (1000–3500 rpm). When the thickness increased from 55 nm to 90 nm, the variation in light reflectance around 375 nm (Fig. 6) ranged from 21% (S1, 88.22 nm thickness) to 10% (S6, 57.62 nm thickness). Moreover, when the thickness of the AR coating increases, the optical path length that the light waves traverse through the coating also increases, which leads to maximizing the peak reflectance.

The reflectance of all samples tends to decline further after the peak point of the spectrum. This may occur due to destructive interference. As the thickness changes, minimum reflectance due to destructive interference occurs at different wavelengths of the samples S1 to S6 in the 300–900 nm wavelength region as shown in Table II.

According to Table II, the minimum reflection was shifted towards a shorter wavelength when thickness was reduced. The minimum reflectance of 2.5% at 570 nm was observed from sample S5, which has a thickness of 63.32 nm. Hence, sample S5 fulfilled the requirement for AR coating having a value closer to the calculated theoretical value (65 nm) in the initial experimental design. This further validated the results of the initial design.

However, according to Fig. 6 and Table II, sample S6 shows greater reflectance than sample S5 despite having lower thickness than S5. As the thickness decreases beyond its optimum value, the coating may become less able to interfere destructively with incoming light waves, resulting in increased reflectance. Therefore, further reduction of the thickness beyond 63.32 nm may not be effective in reducing the reflectance.

Surface Analysis

After identifying the best AR coating for sample S5, further analysis was performed to determine the surface topography and elemental analysis. Figure 8 shows the AFM images of ZnO spin-coated at 3000 rpm (S5). The root-mean-square

Table II Minimum reflectance with corresponding wavelength of the samples S1 to S6

Sample	S1	S2	S3	S4	S5	S6
Thickness (nm)	88.22	81.5	74.3	67.64	63.32	57.62
Wavelength (nm)	735	720	695	690	570	565
Minimum reflectance (%)	4.6	4.1	3.6	3.1	2.5	3.2

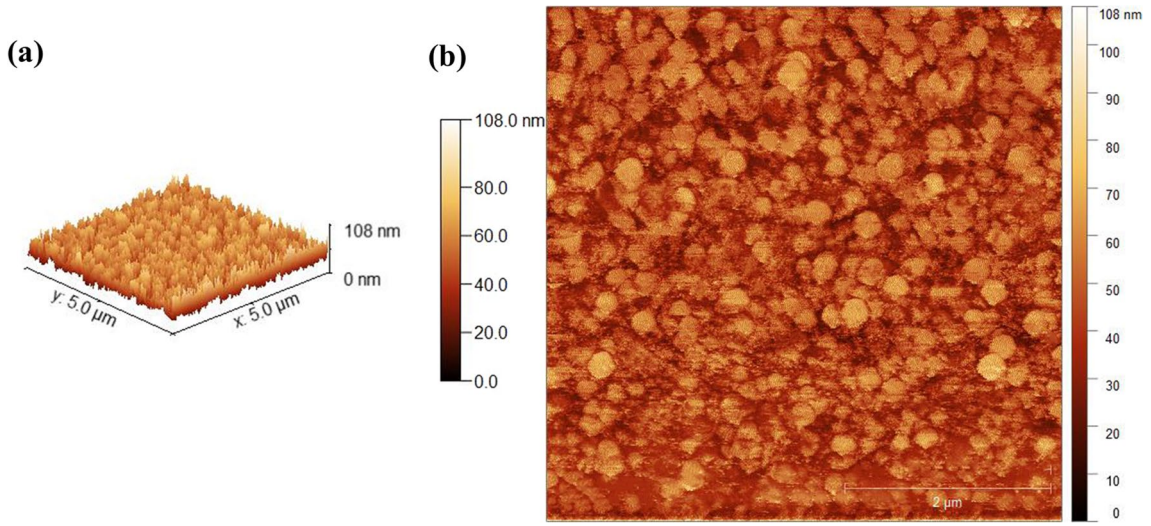

Fig. 8 (a) 3D and (b) 2D AFM images of ZnO surface deposited at 3000 rpm.

Table III Composition of ZnO sample grown on FTO/glass substrate

Element	Weight (%)	Atomic (%)
O	13.75	48.55
Si	5.09	10.23
Sn	74.47	35.44
Zn	6.68	5.77

(RMS) roughness of sample S5 was measured as 11.44 nm, while the roughness of the bare surface was 7.86 nm. Hence, it is evident that the resultant increase in substrate roughness is due to the ZnO AR coating. This AR coating may enhance the light-trapping ability of the device. When light hits the device, some light can be reflected due to the refractive index difference between the two mediums. The presence of a rough surface can cause multiple reflections and increase light entering the device, leading to improved current density and power conversion efficiency.

Elemental Analysis

The composition of the glass/FTO/ZnO substrate is shown in Table III. The ZnO layer was deposited on the FTO layer for convenience of measurement. Accordingly, the formation of ZnO was confirmed.

Device Characterization

The laboratory-developed glass/FTO/CBD-CdS/CSS-CdTe/Cu/Au device[15] was then completed by depositing the AR coating of ZnO following the preparation of sample S5. Three replicates were used for the device performance

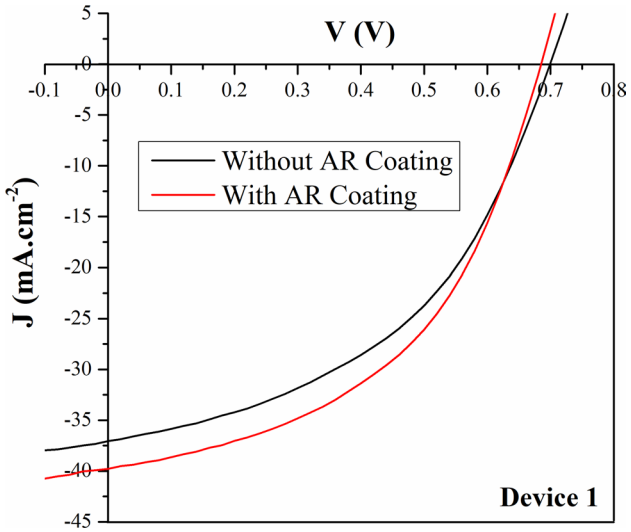

Fig. 9 *J–V* curves for device 1 with and without AR coating.

measurements. Figure 9 shows the current density vs. voltage (*J-V*) curve of one device with and without AR coating. After introducing the AR coating, the light passing through the coating and into the cell increased due to a reduction in reflectance, which allows more photons to absorb into the device, leading to a higher generation of electron-hole pairs. As a result, more charge carriers are available, thereby increasing the current density. Therefore, after deposition of the AR coating, the current density increased from 37.1 mA cm^{-2} to 39.8 mA cm^{-2}, resulting in an increase in PCE from 11.9% to 13.2%.

The experimental findings for additional devices are detailed in Table IV, indicating average improvements in

Table IV Comparison of device performance with and without AR coating

		J_{SC} (mA cm^{-2})	J_{SC} improvement (%)	PCE (%)	PCE improvement (%)
Device 1	Bare	37.1	7.3	11.9	10.9
	With AR	39.8		13.2	
Device 2	Bare	35.5	6.2	13.4	9.0
	With AR	37.7		14.6	
Device 3	Bare	37.2	6.2	13.9	7.9
	With AR	39.8		15.0	
Device 4	Bare	34.8	7.7	12.2	9.8
	With AR	37.6		13.4	
Device 5	Bare	37.2	6.7	13.3	8.2
	With AR	39.7		14.4	
Device 6	Bare	37.7	6.9	12.3	9.8
	With AR	40.3		13.5	
	Average		6.8		9.3

current density and PCE of 6.8% and 9.3%, respectively. The results show that the enhancement in device performance after ZnO single-layer AR coating deposition has surpassed the recorded values in multilayer AR coatings introduced for CdTe-based solar cells.

Conclusion

In this study, optimal conditions for the growth of ZnO AR coating using the spin coating technique were identified as 3000 rpm for 15 s using a zinc acetate precursor dissolved in methanol. Furthermore, minimal reflectance (2.5%) and surface roughness (11.44 nm) confirmed the suitability of the growth of ZnO as an AR coating. Additionally, after introducing the optimized ZnO AR coating, the average current density and power conversion efficiency of the laboratory-developed CdS/CdTe solar cells were enhanced by 6.8% and 9.3%, respectively. Therefore, spin-coated ZnO is an ideal AR coating for CdS/CdTe solar cell devices.

Acknowledgments The authors gratefully acknowledge the support provided by the Senate Research Grant of the University of Moratuwa under Grant Number SRC/LT/2021/08.

Author contributions All authors contributed to the study conception and design. Material preparation, data collection and analysis were performed by J.R. Wijesingha, G.K.U.P. Gajanayake and W.A.V.U. Wickramasinghe. R.M.T Damayanthi, G.I.P De Silva, and D.S.M. De Silva revised the manuscript. The first draft of the manuscript was written by J.R. Wijesingha, and all authors commented on previous versions of the manuscript. All authors read and approved the final manuscript.

Data availability The datasets analyzed during the current study are available from the corresponding author upon reasonable request.

Conflict of interest On behalf of all authors, the corresponding author states that there is no conflict of interest.

References

1. M. Imamzai, M. Aghaei, and Y.H. Thayoob, A review on comparison between traditional silicon solar cells and thin-film CdTe solar cell. *Proc. Natl. Grad. Conf.* 2012, 8 (2011).
2. *Best Research-Cell Efficiency Chart | Photovoltaic Research | NREL*, https://www.nrel.gov/pv/cell-efficiency.html
3. M.A. Green, E.D. Dunlop, M. Yoshita, N. Kopidakis, K. Bothe, G. Siefer, and X. Hao, Solar cell efficiency tables (Version 63). *Prog. Photovoltaics Res. Appl.* 32, 3 (2024).
4. U. Gangopadhyay, K. Kim, D. Mangalaraj, and J. Yi, Low cost CBD ZnS antireflection coating on large area commercial mono-crystalline silicon solar cells. *Appl. Surf. Sci.* 230, 364 (2004).
5. M. Li, H. Shen, L. Zhuang, D. Chen, and X. Liang, SiO_2 antireflection coatings fabricated by electron-beam evaporation for black monocrystalline silicon solar cells. *Int. J. Photoenergy* 2014, 1 (2014).
6. R. Sagar and A. Rao, Increasing the silicon solar cell efficiency with transition metal oxide nano-thin films as anti-reflection coatings. *Mater. Res. Express* 7, 1 (2020).
7. M.Z. Pakhuruddin, Y. Yusof, K. Ibrahim, and A. Abdul Aziz, Fabrication and characterization of zinc oxide anti-reflective coating on flexible thin film microcrystalline silicon solar cell. *Optik (Stuttg)* 124, 5397 (2013).
8. J.-Y. Wang, C.-S. Huang, S.-L. Ou, Y.-S. Cho, and J.-J. Huang, One-step preparation of TiO_2 anti-reflection coating and cover layer by liquid phase deposition for monocrystalline Si PERC solar cell. *Sol. Energy Mater. Sol. Cells* 234, 111433 (2022).
9. P.M. Kaminski, G. Womack, and J.M. Walls, *Broadband Anti-Reflection Coatings for Thin Film Photovoltaics*, in *2014 IEEE 40th Photovoltaic Specialist Conference (PVSC)* (IEEE, 2014), pp. 2778–2783.
10. A.M. Law, L. Kujovic, M. Togay, R.C. Greenhalgh, L.C. Infante-Ortega, X. Liu, and J.M. Walls, A broadband multilayer antireflection coating for thin film CdSeTe/CdTe solar cells. *IEEE J. Photovoltaics* 14, 305 (2024).

11. T.A. Gessert, R.G. Dhere, J.N. Duenow, J.V. Li, S.E. Asher, and M.R. Young, *Comparison of CdS/CdTe Superstrate and Substrate Devices Fabricated with a ZnTe:Cu Contact Interface*, in *2010 35th IEEE Photovoltaic Specialists Conference* (IEEE, 2010), pp. 000335–000339.
12. A.M. Alsaad, Q.M. Al-Bataineh, A.A. Ahmad, Z. Albataineh, and A. Telfah, Optical band gap and refractive index dispersion parameters of boron-doped ZnO thin films: a novel derived mathematical model from the experimental transmission spectra. *Optik (Stuttg)* 211, 164641 (2020).
13. K. Ellmer, A. Klein, and B. Rech eds., *Transparent Conductive Zinc Oxide*. Vol. 104 (Berlin Heidelberg, Berlin, Heidelberg: Springer, 2008).
14. M.M. Diop, A. Diaw, N. Mbengue, O. Ba, M. Diagne, O.A. Niasse, B. Ba, and J. Sarr, Optimization and modeling of antireflective layers for silicon solar cells: in search of optimal materials. *Mater. Sci. Appl.* 09, 705 (2018).
15. G.K.U.P. Gajanayake, A.A.I. Lakmal, D.S.M. De Silva, and B.S. Dassanayake, Effect of CdTe nucleation layer on the performance of CdS/CdTe thin film solar cells. *J. Mater. Sci. Mater. Electron.* 34, 508 (2023).
16. B. Ganesh, K.Y. Rani, B. Satyavathi, and K.S.K.R. Patnaik, Experimental analysis in different batch operating units for process intensification: methyl acetate production case study. *Int. J. Ind. Chem.* 5, 85 (2014).
17. V.N. Jafarova and G.S. Orudzhev, Structural and electronic properties of ZnO: a first-principles density-functional theory study within LDA(GGA) and LDA(GGA)+U methods. *Solid State Commun.* 325, 114166 (2021).